Ultrasonic measurements of undamaged concrete layer thickness in a deteriorated concrete structure

CrossMark

A. Demčenko *, H.A. Visser, R. Akkerman

Chair of Production Technology, Faculty of Engineering Technology, University of Twente, 7500AE Enschede, The Netherlands

ABSTRACT

Ultrasonic wave propagation in deteriorated concrete structures was studied numerically and experimentally. Ultrasonic single-side access immersion pulse-echo and diffuse field measurements were performed in deteriorated concrete structures at 0.5 MHz center frequency. Numerically and experimentally it is shown that the undamaged layer thickness in a deteriorated concrete structure is measurable using pulse-echo measurements when the deterioration depth is larger than the wavelength. The signal overlapping, which occurs in the thin deteriorated layers, can be overcome using diffuse field measurements or a pattern matching technique. The ultrasonic experimental data were shown to be in good agreement with the widely used phenolphthalein test for concrete degradation.

© 2015 Elsevier Ltd. All rights reserved.

1. Introduction

When concrete pipelines are buried in an aggressive soil, the physico-chemical aggressivity of the environment causes deterioration in the concrete; resulting in a decrease in strength of the concrete over time. In the early stages of deterioration a thin deteriorated layer is induced in the concrete structure. In a general case the physico-chemical damage may occur from both sides of the structure: from both internal and external surfaces [1]. Therefore, a measurement technique, used for the inspection of deteriorated concrete structures, must work reliably at different inspection conditions: from both the undamaged and the deteriorated side of the structure. Various inspection techniques such as visual, electromagnetics, acoustics and ultrasonics are used for concrete structure testing [2–4]. Acoustic methods are especially attractive for inspection of water mains due to the possibility of immersion ultrasonic measurements from the inside. Hence, the measurements are contactless and suitable for automatic robotic scanning.

Ultrasonic measurements have been widely used for the characterization of concrete structures for a long time, for example, see the reported work [5] which presents the characterization of concrete structures by means of the analysis of the speed of ultrasonic pulse propagation. The ultrasonic frequency range used for concrete characterization, depends on the following conditions: (a) concrete structure or/and concrete mixture (including its aggregate size), (b) structural thickness, and (c) measurement method. Therefore, the frequency of the ultrasonic wave must be selected according to the measurement conditions very carefully. It is necessary to use high frequency ultrasonics in the frequency range of 0.5–1 MHz to detect the early stages of deterioration in concrete and to measure thin deteriorated layers using conventional ultrasonics such as pulse-echo technique [6]. However, to perform measurements at high frequencies, for example at 1 MHz center frequency, is complicated when a deteriorated layer is present in the concrete structure. The difficulties arise due to the high acoustic losses which exist in the deteriorated concrete layer and these losses are caused by high scattering. In the reported work [6] the through-transmission measurement mode was used, and this measurement mode enabled the signal to noise ratio to be improved. However, through-transmission measurements are not suitable for inspection of buried pipes or other structures when only a single-side access to the structure is possible.

As an alternative to bulk wave ultrasonic techniques, different acoustic measurements have been used for the characterization of concrete deterioration. For example, different guided wave techniques have been used such as the surface wave technique which is limited to the measurement of the accessible surface of the structure [3,7,8] (therefore it is not analyzed in detail in this study) and the guided ultrasonic technique [2,9]. The latter technique is attractive for field inspections, because the guided waves may propagate over a long range (up to a few hundred meters). However, with this technique the detection of local low level deterioration zones is questionable. Moreover, with the current state of the technique it is only possible to determine an average status of

the concrete structure within the inspection region. However, low frequency guided waves can be used over a short range [10]. But in this case to generate a single guided wave mode becomes difficult, therefore it is complicated to utilize this kind of technique for field measurements when only single-side access to a structure is allowed [10]. A low density of the deteriorated concrete also causes problems for the use of guided ultrasonics for inspection of the buried concrete pipes. The density of the deteriorated concrete may become close to the density of the soil, therefore Cremer's principle is not valid anymore [11]. Practically this means that the propagation of the guided waves will depend on the acoustic loading. For example, the properties of the soil will affect the guided wave propagation in the buried pipe case.

Recently developed acoustic techniques, used for evaluation of concrete properties, have investigated various nonlinear ultrasonic techniques such as harmonic generation [12], wave mixing [13] and diffuse field techniques [14–20]. The use of nonlinear ultrasonics for concrete inspection is attractive due to the high non-linearity of the concrete and very high sensitivity of the nonlinear ultrasonics to various types of damage. Usually the nonlinearity of the concrete is one order higher than in metals [21]. However, it is difficult to implement nonlinear ultrasonics measurements based on the harmonic generation due to various parasitic nonlinearities which distort the received harmonics. Wave mixing techniques can be used to overcome these distortions, but it requires a more sophisticated and complex acoustic configuration for the experiments [22,23].

Diffuse field measurements also demonstrate a very high sensitivity to material changes. The simplicity of a practical realization of a diffuse field acoustic measurement makes this technique more attractive for practical measurements than the application of nonlinear ultrasonics. First of all, the diffuse field technique does not require the ultrasonic transducers to be oriented at a specific angle, i.e. the inclination of the transducers is perpendicular to object's surface. Secondly, it is easy to combine the diffuse field measurements with pulse-echo measurements, i.e. the same acoustic measurement configuration can be used during both experiments.

Single-side access immersion ultrasonic measurements of the undamaged concrete layer thickness in deteriorated concrete structures is the key issue of this study. Pulse-echo and diffuse field measurements are performed at a center frequency of 0.5 MHz on concrete specimens. The pulse-echo measurement results from the test specimens are verified by the standard phenolphthalein tests [24] and pattern matching technique [25].

This paper is structured as follows. The opening two sections describe the preparation procedure which was used for the production of the concrete specimens with different deterioration levels and presents the two ultrasonic measurement methods, used for the evaluation of the concrete. Then initial non-acoustic and acoustic characterizations of undamaged and deteriorated concrete specimens are presented. Next to the measured material properties, a multi-layered wave propagation model is utilized for prediction of ultrasonic signals reflected from the deteriorated concrete specimens at different deterioration conditions is presented. Subsequently the experimental results for pulse-echo and diffuse field measurements are presented. Finally, the phenolphthalein test results of the concrete deterioration are presented and compared with the acoustic results and numerical predictions.

2. Specimens

9 specimens were prepared from components listed in Table 1. The specimens had approximate dimensions 30 mm × 100 mm × 290 mm. An HCl acid solution of 20% was used to induce and

Table 1
Concrete mixture components by ratio of mass fraction. Fine quartz sand is from the current Dutch stock.

	Cement	Quartz sand	Water	Plasticizer
Ratio	1	0.5685	0.2041	0.0026

Table 2
Concrete treatment time by the 20% HCl acid solution. The reference specimen is not listed in the table.

Time, h	Single-sided deteriorated	168	336	504	672	1008
	Double-sided deteriorated for each side		336	504	672	

accelerate a chemical deterioration in the concrete specimens [26] (for the description of the chemical reactions occurring, see [27]). In the reported work [28] an analysis of concrete mechanical properties when the concrete is deteriorated using HCl solution is presented.

The following procedure was used for the concrete treatment by the acid solution. A single-side of a raw concrete specimen was kept in a box with the acid solution. The box contained 0.5 l of the acid solution. A partial immersion of the specimens was achieved in this way, keeping the un-immersed side in air. The specimen submersion depth was 14–15 mm. The specimens were kept for at least one week in the acid solution. After this, the specimens were washed with fresh water and some specimens were immersed in a fresh acid solution for another week. In this way, concrete specimens with different deterioration levels were produced. The concrete treatment time by the acid solution is listed in Table 2.

Single-sided and double-sided deteriorated concrete specimens were prepared (see Table 2) for investigation of different measurement conditions. The double-sided deterioration specimens were kept in the acid solution identical time periods from both sides. Each side of the specimen was immersed into the acid solution separately. During the treatment of the second surface of the concrete specimen, it was found that the first deteriorated surface became wet in air. This never happened for the single-sided deteriorated specimens. The wetting of the un-immersed surfaces was attributed to the acid propagation via micro-capillaries which were formed by the acid treatment of the first surface.

3. Ultrasonic measurement methods

Two different ultrasonic measurement methods are used in the measurement of the undamaged layer thickness in the concrete specimens: (a) pulse-echo and (b) diffuse field technique. Both measurement configurations are presented in Fig. 1. Due to the advantages of immersion based ultrasonic measurement techniques, the experiments are performed in a water tank employing an ultrasonic scanner. B-scanning measurements were performed at the center part of the specimens (see Fig. 1, dark gray area). A step size of 1 mm is used in the scanning direction.

The pulse-echo measurement configuration, which involves a single ultrasonic transducer operating in transmission and reception modes, (Fig. 1(a)) is attractive for industrial measurements due to its simplicity in practical implementation and signal processing. However, this measurement configuration has a limited discriminating capacity for the estimation of the structural state of the concrete. The limitations of the pulse-echo measurement configuration are presented and discussed in section *V*.
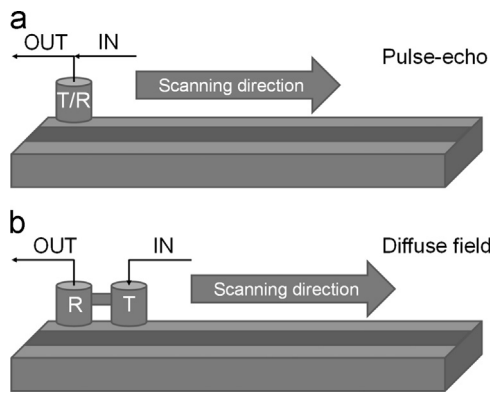
Fig. 1. Ultrasonic pulse-echo (a) and diffuse field (b) measurement configurations, where T and R being the transmitter and receiver, respectively.
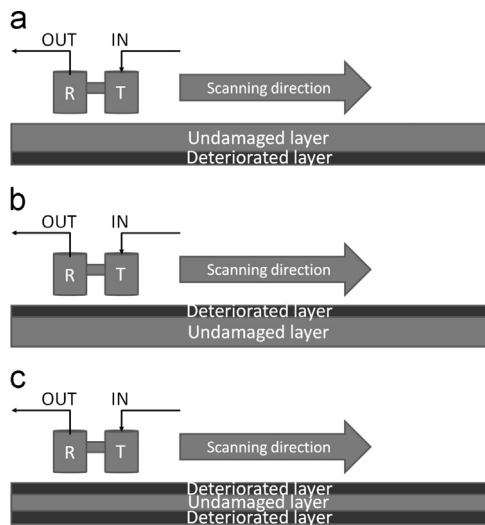

Fig. 2. A schematic arrangement of the ultrasonic measurements performed at deteriorated concrete specimens: (a) from the undamaged side, (b) from the damaged side, and (c) from both sides of double-sided deteriorated specimens.

The diffuse field measurement technique is used as an alternative to the pulse-echo measurements. This technique involves two ultrasonic transducers (see Fig. 1(b)). Each transducer operates in a single mode: transmission or reception. This is a relatively simple configuration of the acoustic measurement, for example, it does not require special inclination angles for the transducers, which makes this technique attractive for industrial measurements, too. However, in this case signal processing is somewhat more complicated when compared to the pulse-echo case. The pulse-echo and diffuse field techniques differ in their wave propagation ranges. The pulse-echo measurement is performed at a single point, and the measurement covers the region of the beam directly below the ultrasonic transducer. The diffuse field measurement is performed over a certain range of the structure under inspection, i.e. in the range which is between the two transducers (see Fig. 1(b)). Therefore, a larger coverage of the structure under inspection is achieved with a single measurement. It is also important to note that the diffuse field measurement technique can easily be combined with the pulse-echo technique, because the transmitter simultaneously may work in the wave reception mode.

The specimen arrangements studied in the experiments are shown in Fig. 2. With the combination of these arrangements all possible concrete access cases are covered: access to the concrete structure from the undamaged (Fig. 2(a)) or the damaged (Fig. 2(b

and c)) side. When the concrete structure is deteriorated from both sides, the measurements are performed for each side separately. It is seen that the deteriorated concrete specimen becomes a structure consisting of two or three layers, therefore the evaluation of these structures is more complicated than in the single-layered material case.

4. Initial characterization of test specimens

After deterioration of the concrete specimens by the HCL acid solution, the specimens were weighed. The relative weight change is shown in Fig. 3. However, these measurement results are approximate, because the deteriorated concrete becomes soft making them susceptible to physical damage of the deteriorated specimen. The measured density is $\rho_0 = 2270$ kg/m^3 in the undamaged specimen, and the density of the damaged layer was determined from the change of the weight employing the following equation:

$$\rho_d = \frac{m_1 - (V_0 - V_1)\rho_0}{V_1}, \tag{1}$$

where m_1 is the weight of the specimen after the treatment by the acid, V_0 is the volume of the specimen, V_1 is the volume of the deteriorated part of the specimen. The calculated density is 1325 kg/m^3 in the deteriorated part of the specimen.

From Fig. 3 it can be seen that the weight change has a linear trend with time. The double-sided deterioration results show that, as expected, the weight change is almost double that of the single-sided deteriorated specimens. In the literature various rates of weight loss are reported, including proportional to square root of time [29] and linear [4,26].

Initially B-scanning is performed on the undamaged concrete specimen to estimate longitudinal wave phase velocity in the specimens. A 0.5 MHz center frequency planar ultrasonic transducer with a diameter 25 mm was used in the immersion measurements and used in pulse-echo measurement mode (see Fig. 1(a)). A single rectangular pulse excitation was used in all measurements. A distance of 70 mm was maintained between the transducer and specimen surfaces. From the collected data, the phase velocity (c_{ph}) of the longitudinal wave in the specimen is estimated using the phase-spectrum method [30]. The phase velocity experimental data are averaged in the frequency domain, due to the expected scattering of ultrasonic signals in the concrete. The processed results including standard deviations are presented in Fig. 4. Each averaged data point is the result of 208 different
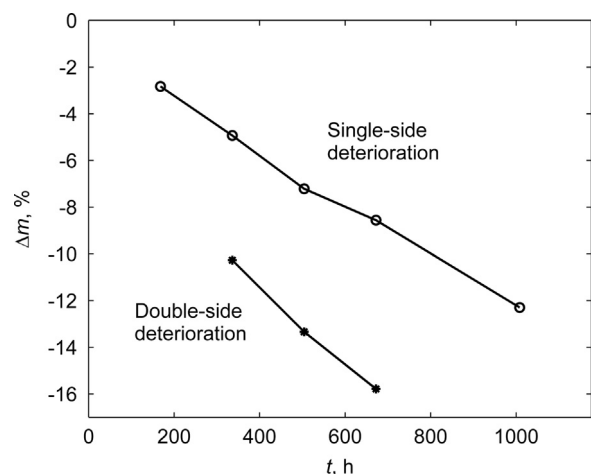

Fig. 3. Relative weight change of concrete specimens due to different 20% HCl acid solution treatment time.
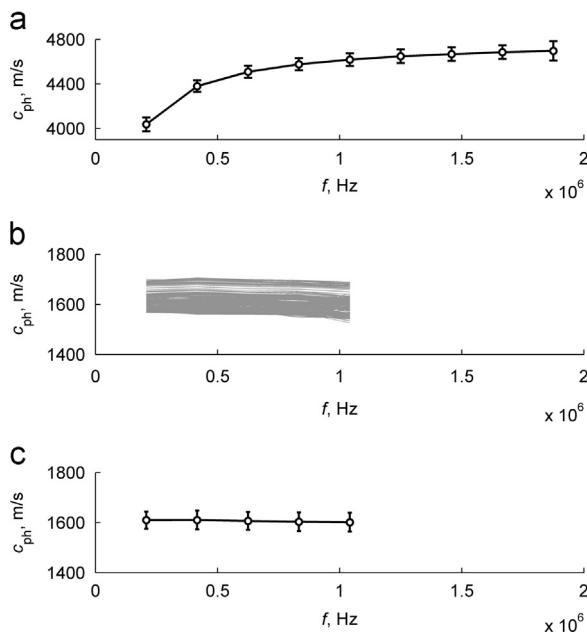
Fig. 4. Measured longitudinal wave phase velocity in the undamaged (a) and damaged (b and c) concrete specimens. The phase velocity measured dispersion curves in the deteriorated concrete specimen: individual curves at each measurement point (b) and averaged dispersion curve (c). The error-bars show the standard deviations.

measurement points on the concrete specimen. The mean standard deviations is estimated to be 60 m/s.

A measurement of the phase velocity becomes more complicated in the deteriorated concrete layer due to an increased porosity in the specimen. These measurements are performed on the single-sided deteriorated specimen which is kept in the HCl acid solution for 1008 h. Initially, an undamaged layer thickness is measured in the specimen from the undamaged side. From the measured data it is found that the damaged layer thickness is about 8 mm (true value is 7.74 mm ± 0.39 mm). The B-scan is performed from the deteriorated layer side (Fig. 2(b)) and it is found that the damaged layer thickness is about 8 mm (true value is 7.93 mm ± 0.36 mm). When all ultrasonic experiments were completed, the specimen was cut along B-scan axis and the thickness was measured mechanically using a caliper. The mechanically measured thickness was 7.9 mm ± 0.2 mm. Hence, it is assumed that the deterioration layer thickness is uniform and it is 8 mm during extraction of the phase velocity from the experimental data using the phase-spectrum method.

Fig. 4(b) depicts the estimated phase velocity dispersion curves of the longitudinal wave in the deteriorated layer of the concrete specimen. It is seen that the phase velocity has a very little dispersion in the measured frequency range and the dispersion is slightly negative [31]. Here, 205 measurement points are included in the averaged result (Fig. 4(c)) for the concrete specimen. The corresponding standard deviation is 44 m/s. However, the obtained standard deviation is approximate, because the deterioration depth slightly varies from point to point, whereas the depth level is assumed to be a constant during the measurements of the phase velocity. From the dispersion measurement results it is seen that the deteriorated concrete behaves as a two phase material in the analyzed frequency range. More information about the phase velocity behavior in porous materials is presented in [31,32].

From the experimental data the following group velocities of the longitudinal wave at the center frequency of 0.5 MHz are estimated: 4800 m/s and 1620 m/s in the undamaged and

deteriorated concrete, respectively. A cross-correlation technique is used for the estimation of time of flight of acoustic signals to calculate the group velocity by searching for the maximum correlation coefficient. It is seen (see Fig. 4 for the phase velocity value at 0. 5 MHz frequency) that the group velocity is higher than the corresponding phase velocity in the undamaged specimen. The corresponding difference is 380 m/s. In the deteriorated concrete case the corresponding difference is −20 m/s, i.e. the group velocity is below the phase velocity at the 0.5 MHz frequency. This small difference confirms that the dispersion is very small in the analyzed frequency range. In this study the group velocity, estimated by a cross-correlation technique, is used to measure the deterioration level in the concrete specimens.

The wavelength λ can be calculated from the measured phase velocity in the concrete specimens with $\lambda = c_{ph}/f$, where c_{ph} and f are the phase velocity and frequency of the wave, respectively. The corresponding wavelengths are 8.8 mm and 3.2 mm in the undamaged and deteriorated concrete specimens, respectively, at 0.5 MHz center frequency.

Ultrasonic wave attenuation is not analyzed for the concrete specimens, because they have a high local variation and it is difficult to use them for the estimation of concrete deterioration level. However, it is useful to note that the attenuation is much higher in the deteriorated layer than in the undamaged concrete. The higher attenuation is thought to be caused by an increase in the porosity of the deteriorated concrete.

5. Numerical prediction and analysis of ultrasonic signals in a deteriorated concrete structure

A physico-chemical aggressive environment may induce a single-sided or double-sided deterioration of the concrete structure. In the previous section it is shown that material properties between the undamaged and damaged layers differ significantly. Therefore, the damaged concrete structure is analyzed as a double layered (for single-sided deterioration) or triple layered structure (for double-sided deterioration) with the corresponding material properties. The situation with a transient layer (in our analysis linearly graded properties were employed to analyze this situation) has been analyzed numerically, but these results were not presented in the final form of the manuscript (due to length considerations). It can be shown that the transient layer starts to play a role when its thickness is comparable with the ultrasonic wavelength. In this study the stiffness matrix method [33] is used to model the ultrasonic waves in the layered structures. Using this method, the reflection coefficients of ultrasonic signals are predicted from the layered concrete structure immersed in water. Finally, ultrasonic signals are calculated using the procedure presented in [34].

The following constraints are introduced to simplify the modelling: (a) the receiver is assumed to be a plane wave source, and (b) each structure layer (undamaged and deteriorated) is assumed to be homogenous and their properties are frequency independent. The first constraint is valid in our case, because this study is dedicated to the thickness measurements and the inclination angle of the ultrasonic transducer is perpendicular to the surface of measured object. Therefore, the prediction of the time of flight of ultrasonic signals, which provides information about the thickness of the separate layers, is more important than a prediction of absolute amplitude of ultrasonic signal. When it is necessary to predict a waveform more accurately, more advanced modeling can be employed which takes a finite dimension of the ultrasonic probe and a specific inclination angle of the probe into account [33]. The second introduced constraint enables the effective concrete properties which are estimated from corresponding averaged material properties to be analyzed.

This constraint neglects the local variations in the material properties, which are present in the material. The dispersion is neglected, because in our case waves propagate over a short range. Finally, the predicted ultrasonic signal is represented via the inverse discrete Fourier transform [35].

The used material properties, Lamé constants and material density, are listed in Table 3. In this work the value for the shear modulus μ is measured using the noncollinear wave mixing approach [36] in the undamaged concrete specimen. The shear modulus is chosen arbitrarily for the deteriorated concrete specimens. It is useful to note that that the measurements were conducted without rotation of ultrasonic transducer (inclination angle 0 degree), and only the stiffness constant $c_{33} = \lambda + 2\mu$ was involved in the ultrasonic response of the longitudinal wave. The ultrasonic attenuation is introduced via complex stiffness constants, to keep the predicted amplitudes proportional to the experimental results. The imaginary parts are estimated using a trial and error approach, i.e. minimizing the difference between the predicted and experimental results.

For the prediction of ultrasonic signals, the following parameters are used as a 1D model input:

(1) The number of layers in a solid structure. For the undamaged concrete structure there will be only one layer; two layers for a single-sided deteriorated structure and three layers in a double-sided deteriorated concrete structure.
(2) Viscoelastic properties and material density of each solid layer (see Table 3);
(3) Thickness of each layer;
(4) Ultrasonic wave incident angle (in this study it is fixed and it is 0 degree);
(5) Analyzed frequency interval;
(6) Surrounding material properties (in the present case it is water, see Table 3);
(7) Initial ultrasonic signal emitted by ultrasonic transmitter.

By varying the model input parameters, it is possible to model different measurement conditions such as different deterioration depth of the concrete or different material properties of the concrete.

The experimentally obtained and predicted ultrasonic signals at a 0.5 MHz center frequency are shown in Fig. 5. Fig. 5(a and b) depict the following typical ultrasonic signals: reflected signals when the measurements are performed from the undamaged and deteriorated sides of the specimen (1008 h in HCl solution), respectively. Fig. 5(c) shows results when the predictions and measurements are performed in the double-sided deteriorated specimen (576 h in HCl solution). It is seen that a very good correspondence is obtained between the predicted (gray signals) and experimental signals (black signals) (Fig. 5(a and b)). A disparity between the signals (see Fig. 5(c), the third and the fourth reflections) is caused due to different deteriorated layer thickness in the experimental specimen. The difference of the deterioration thickness could be caused by HCl solution which penetrated the un-immersed surface via micro-capillaries. In the figure the experimental signals are obtained from corresponding averaged experimental B-scan data. It is useful to note that four reflected ultrasonic pulses can be determined in the raw acoustic signal with a reasonable signal to noise level.

A time-of-flight of the ultrasonic signals (see Fig. 5) is analyzed to interpret the ultrasonic response from the deteriorated concrete specimens. Knowing the wave velocities in the corresponding concrete layers (undamaged and deteriorated), a periodicity of the time instants are calculated for each possible re-reflected signal. The time-of-flight analysis shows that a bottom surface reflection (damaged layer) is not observed in the analyzed case (see Fig. 5 (a)). Multiple re-reflected ultrasonic signal within the undamaged layer are presented in the ultrasonic response, only. Fig. 5(b) also clearly indicates that the re-reflected signals within the deteriorated concrete layer are not seen in the ultrasonic response. Fig. 5 (c) shows the ultrasonic response from the two-side deteriorated
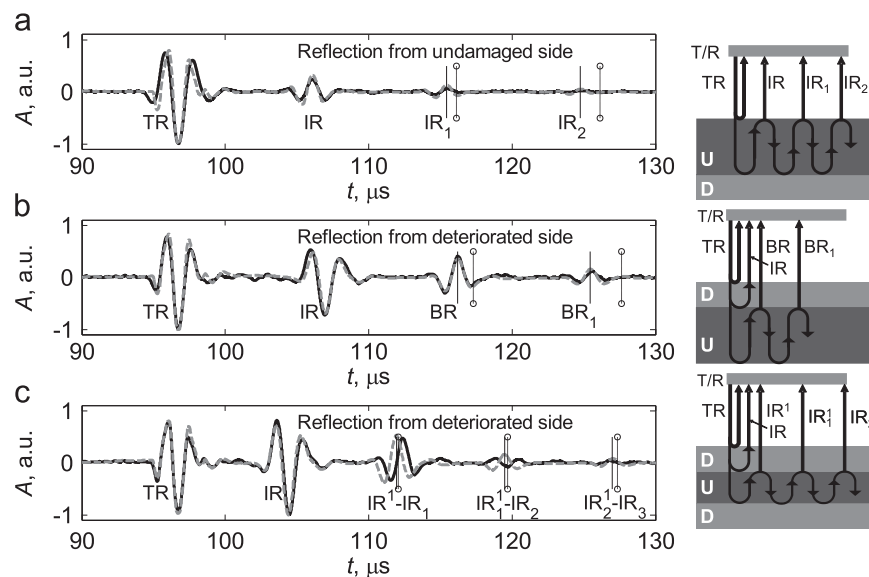
Table 3
Material properties used in the modeling of reflection coefficients.

	λ_e, (GPa)	μ, (GPa)	ρ, (kg/m^3)
Undamaged concrete	29.52–i0.29	11.39–i0.11	2270
Deteriorated concrete	0.29–i0.03	1.60–i0.15	1325
Water, $c_f = 1480$ m/s			1000

Fig. 5. Predicted (dashed gray) and experimental (black) reflected signals from the deteriorated concrete specimens in pulse-echo mode: (a) reflection from undamaged side, (b) reflection from deteriorated side, (c) reflection from deteriorated side when both sides are damaged. The signals are scaled by their maximum values. Solid vertical lines indicate the time instants of the multiple re-reflections within the undamaged concrete layer. Vertical lines with circles indicate the time instants of the multiple re-reflections within the deteriorated concrete layer. Intermediate reflections are not shown. TR is the reflection from the top surface, IR is the reflection from the interface, BR is the reflection from the bottom surface of the second layer. D and U denote the deteriorated and undamaged concrete layers, respectively.

concrete structure. It is seen that both time instants (multiples of the re-reflected signals within the deteriorated and undamaged concrete layers) are very close to each other, i.e. an overlapping of the signals occurs. However, previously analyzed cases (Fig. 5(a and b)) show that a re-reflection of the ultrasonic signal within the deteriorated concrete layer is not presented in a signal. Moreover, the time instants of the re-reflections within the undamaged layer coincident with peaks of ultrasonic signals. Therefore, it is possible to assume that the re-reflections of the ultrasonic signal within the undamaged concrete layer are presented in the signal shown in Fig. 5(c).

A good temporal separation of ultrasonic signals is obtained when the thickness of a measured layer is a few times larger than the wavelength. If the thickness and wavelength become equivalent, an overlapping of the signals occurs. Therefore, the accurate measurement of the layer thickness becomes complicated or impossible.

6. Pulse-echo measurement results

Fig. 6 shows pulse-echo measurement results of the undamaged layer thickness in the single-sided deteriorated concrete specimens when the experiments are performed at 0.5 MHz center frequency. A distance of 70 mm is maintained between the top specimen surface and transducer surface in the experiments. 231 points are measured in each specimen, i.e. B-scans are performed with a scanning step of 1 mm. Large measurement errors caused by surface defects and/or voids in the specimens are removed from the presented results.

Fig. 6(a) depicts the measurement results from the undamaged and deteriorated sides of the specimens. TR and IR reflections are

used for the thickness determination of the undamaged layer in the concrete structures from the undamaged side of the specimens. IR and BR reflections are analyzed for the undamaged layer thickness measurements when the measurements are performed from the deteriorated side. In both cases the undamaged concrete layer thickness is expressed in the following form:

$$h = 0.5c_{gu}\Delta t_{TR-IR;\ IR-BR}, \qquad (2)$$

where c_{gu} is the group velocity of ultrasonic wave in the undamaged concrete specimen, Δt is time of flight between the corresponding ultrasonic signals in the undamaged concrete layer.

The standard deviation of the results shows a low scattering of the data (Fig. 6(a)). In the worst case the scattering is less than ± 0.5 mm. A good matching of the experimental results is obtained between the measurements from opposite sides. A small difference in the measurement results is caused by a variation of the measurement points (specimens were positioned arbitrarily when changing for the measurement side) and by the measurements itself. In the first case, the thickness is measured employing the ultrasonic signals which propagate in the homogenous material, i.e. in the undamaged concrete layer. Therefore, their wave shapes are identical. When the measurements are performed from the deteriorated side, the wave shapes of the informative signals (IR and BR) are slightly different. This is caused by a significant difference in the material properties of the deteriorated and undamaged layers in the concrete structure (see Table 3). When ultrasonic wave propagates within the damaged concrete layer, higher frequency components of the ultrasonic wave have much higher losses than the lower frequency components, therefore the lower frequency components start to dominate in the signal. This domination causes a difference between wave shapes of the ultrasonic waves in the damaged and undamaged concrete layers, respectively.

The thickness of the deteriorated layer is measured from the deteriorated side of the specimens, to verify different measurement possibilities. After that, the undamaged layer thickness is recalculated from the following equation:

$$h = h_0 - 0.5c_{gd}\Delta\tilde{t}_{TR-IR}, \qquad (3)$$

where h_0 is the full thickness of concrete structure, c_{gd} is the group velocity of ultrasonic wave in the deteriorated concrete specimen, $\Delta\tilde{t}$ is time of flight between the corresponding ultrasonic signals in the undamaged concrete layer.

The undamaged concrete thickness measurement results from Eq. (2) (black color data) together with the thickness results from the IR and BR signals (gray color data) are presented in Fig. 6(b). The experiments prove that it is valid to use Eq. (2) in case signal overlapping does not occur, i.e. if the deterioration depth becomes larger than the wavelength. One can see that the signal overlapping increases scattering of the measurement data and moreover, the interpretation of the measurement results becomes complicated and hence cannot be reliably used. In the presented results the thickness of the undamaged concrete is estimated employing TR and BR signals where the signal overlapping occurs and it is not possible to separate the echo signals from the different interfaces. It means that the ultrasonic measurements do not detect the deterioration in the concrete, hence it is assumed that the concrete structure is undamaged.

A difference which is seen between the two measurement results (Fig. 6(b)) is mostly caused by a thickness variation in the deteriorated layers.

The measurement of the undamaged layer thickness are performed from both sides of the specimens in the double-sided deteriorated concrete structures. The experimental results are shown in Fig. 6(c). Two ultrasonic signals, reflected from top and bottom interfaces of the undamaged concrete layer are used in the
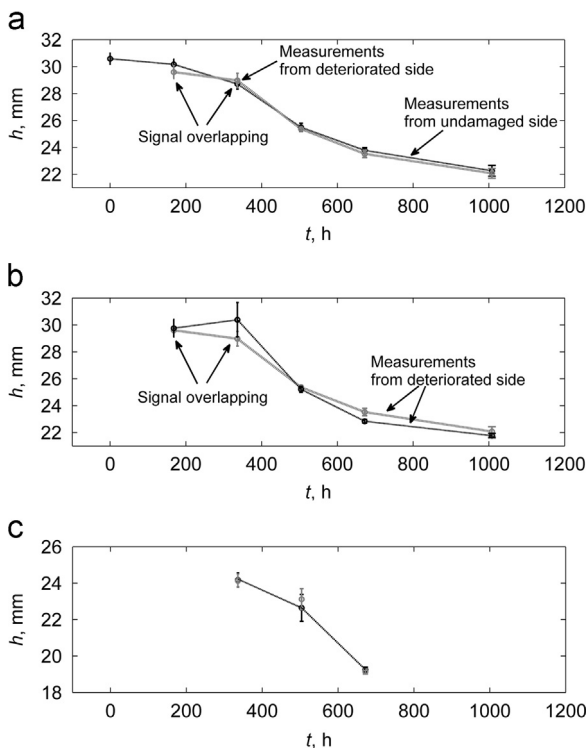

Fig. 6. Measured undamaged layer thickness in the deteriorated concrete specimens: measurements are performed from both sides of the specimens (Eq. (2)) (a), and from the deteriorated side employing measurements of the deteriorated layer thickness (Eq. (3)) (black color data) (b). Pulse-echo measurement results of the undamaged layer thickness in the double-sided deteriorated concrete specimens (c), where the gray and black colors mark the measurement results from two opposite sides of the specimens.

measurements. The experimental results show a low scatter of the data. Only for the second specimen the scattering is higher due to poorer surface conditions in comparison with the other two specimens. In this case the standard deviation of the thickness measurements is ± 0.74 mm. The gray colored data show the measurement results from the specimen side which is first treated by the HCl acid solution and the black color marks the results measured from the second side.

7. Diffuse field measurement results

A typical main part of a diffuse field signal is shown in Fig. 7. The signals are recorded from (a) the reference concrete specimen and (b) the single-sided deteriorated concrete specimen (1008 h in HCl solution) when the measurement is performed from the deteriorated side. It is seen that the informative part duration of the signal is about 92 μs. Longer duration diffuse field signals are not analyzed in this work, because it is difficult to record long acoustic signals without distortions which are caused by various reflections. The focus here is on finding a correlation between a diffuse field parameter and the deterioration layer thickness rather than on estimating absolute values of the diffuse field parameters such as dissipation and diffusivity. It is difficult to estimate the absolute diffuse field parameters due to signal sensitivity to transducer and specimen mounting variations [37].

The signal measured from the deteriorated concrete side (Fig. 7 (b)) clearly shows that the higher frequency components are filtered out due to the high acoustic losses in the deteriorated concrete layer. These high losses limit the separation distance between the transmitter and receiver.

Usually a spectral technique is applied to extract informative signal features. In this study two features of the diffuse field parameters are used for the interpretation of the experimental results: the parameter E and the 2D cross-correlation coefficient. The 2D cross-correlation coefficient is calculated between the time-frequency surfaces of the diffuse field signals. The parameter E is given by

$$E = \sum_{i=1}^{k} \max\left(\mathbf{S} \times \mathbf{S}^{T}\right),\tag{4}$$
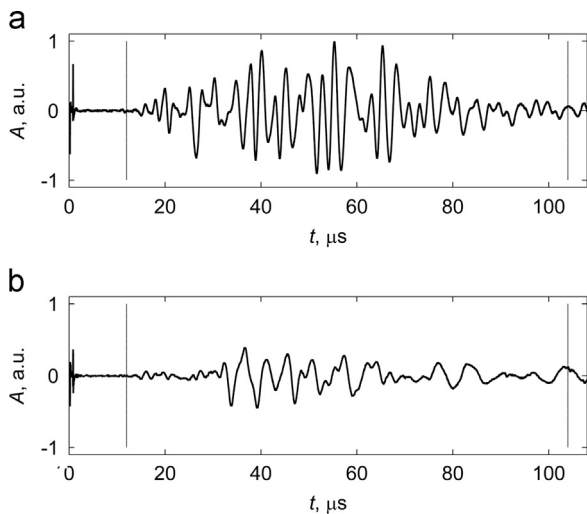

Fig. 7. Typical main part of diffuse field signal at 0.5 MHz center frequency measured from the reference concrete specimen (a) and deteriorated concrete (b). The last signal is measured from the deterioration side of the single-sided deteriorated concrete (1008 h in HCl solution). Vertical lines show the informative part of the signal. The signals are scaled by a maximum value of the reference signal.

where T denotes the transpose of the matrix $\mathbf{S}$, which represents the discrete signal in the time-frequency domain. $\mathbf{S}$ is calculated using a short-time Fourier transform with 80% overlap of segments. The segments are calculated using a Hanning window of 10.4856 μs duration. k is the number of data points. After multiplication of the matrices $\mathbf{S}$, the matrix dimensions become $k \times k$. Finally, the maximum value is found in each column of the matrix, and these maxima are summed. However, other features can also be used for parameterization of the diffuse field signals. For example, see the reported works [17,37].

The correlation between the diffuse field parameters and the deterioration layer thickness in the concrete specimens are demonstrated by representing the measurement results as a relative change of the mean value in the particular diffuse field parameter

$$\Delta x = \frac{\overline{x} - \overline{x}_R}{\overline{x}_R} \times 100\%.\tag{5}$$

Here $x = E, R$. $\overline{x}_R$ is the mean value of the reference parameter, $\overline{x}$ is the mean measured value of the parameter. The reference parameters are measured from the undamaged concrete specimen. An arbitrarily chosen signal is used as the reference in the calculations of 2D cross-correlation coefficient.

Two 0.5 MHz center frequency ultrasonic probes of 25 mm diameter were used in the measurements ($fh = 15$, where is f is the frequency and h is the specimen thickness). In the experiments a distance of 55 mm was maintained between the ultrasonic transducers. The distance between the transducers and specimens was maintained at 10 mm. A single pulse was used for excitation of acoustic diffuse field. A 40 dB gain was applied for amplification of the received signals. The received acoustic signals were averaged across 16 signals. The frequency range between the 0.5 MHz and 1 MHz was used in this study for the extraction of the diffuse field features. The higher frequency bandwidth relative to the center frequency of the incident wave was selected for the parameterization of the diffuse field signals due to the higher influence of the concrete deterioration on the shorter wavelengths (see Fig. 7).

Fig. 8 shows experimental results when the diffuse field measurements are performed on single-sided deteriorated concrete specimens from the undamaged and deteriorated sides, respectively. A good correspondence is obtained between the results for the measurements from both specimen sides: undamaged and deteriorated. The diffuse field measurements show a very high sensitivity to the concrete deterioration when the deterioration depth is less than the wavelength (see the measurement results for the first two specimens with the damaged layers). A validation of ultrasonic measurements is presented in section VIII. For the second specimen (around 300 h), the relative changes of the parameters depending on the measurement side are in the range of 47–67% and 58–67%, for the E and R coefficients, respectively. This is a much higher change than obtained in the pulse-echo measurements (see Fig. 6, signal overlapping zone).

When the deterioration depth further increases in the concrete, a smaller change is observed in the diffuse field parameters (see Fig. 8 and measurement points between 600 h and 1000 h). This saturation indicates that the diffuse field measurements or our chosen parameter becomes ineffective when the deterioration depth is much higher than the wavelength.

Fig. 8(c and d) represent measurement results when the measurements are performed in the double-sided deteriorated concrete specimens. It is seen that the measured differences are small, i.e. almost a saturation is achieved. Therefore it can be difficult to distinguish between the different deterioration levels in field measurements. However, the diffuse field technique works well as a detector of concrete deterioration.
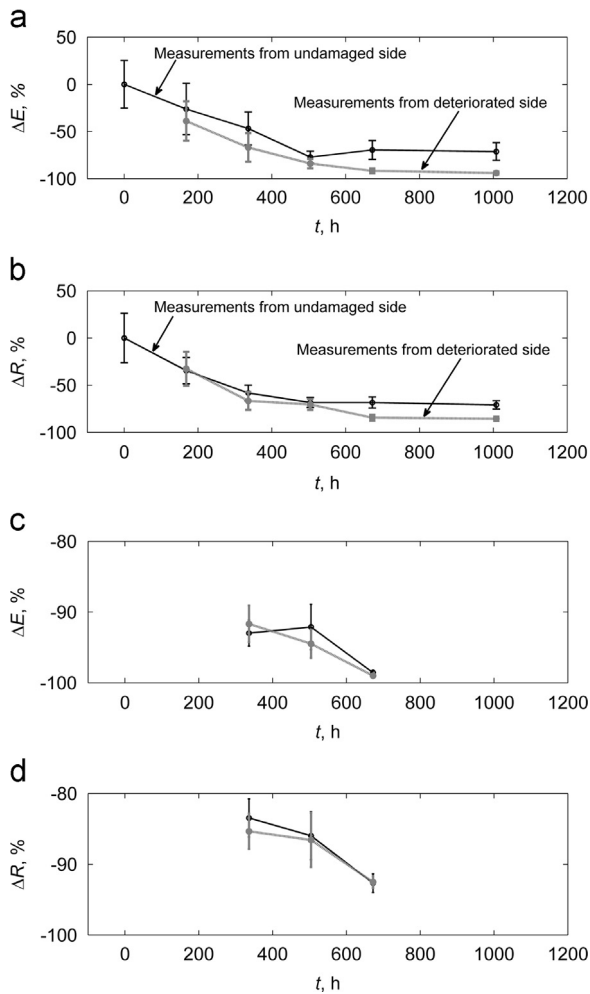
Fig. 8. Relative change of spectrogram parameter E (a and c) and 2D cross-correlation coefficient (b and d) when the diffuse field measurements are performed in the single-sided and double-sided deteriorated concrete specimens, respectively. The gray and black colors indicate measurements performed from the different sides of the specimens.

To summarize, the pulse-echo measurements provide sufficient information about the undamaged concrete layer thickness when the deterioration depth is more than the wavelength. When the deterioration depth is less than the wavelength, it is preferable to use the diffuse field technique. Moreover, the diffuse field technique can be employed for detection of cracks in concrete, for example, see the reported works [17,18].

The diffuse field measurement results (see Fig. 8) show a higher data scatter than in the pulse-echo measurement case. It can be seen that the scattering decreases when the deterioration depth in the concrete increases. This decrease is caused by a lower frequency bandwidth of the diffuse field signals in the deteriorated concrete specimens when the deterioration becomes more significant. It means that most of acoustic signal energy is transported at the lower frequency (hence the ultrasonic signal is less sensitive to intrinsic microstructure variations in the concrete) which provides more stable amplitude of ultrasonic signals.

8. Verification of ultrasonic measurement results using phenolphthalein test and pattern matching technique

The standard Phenolphthalein test was performed for the deteriorated concrete specimens. For this purpose, each specimen

was cut along the center. After that the phenolphthalein was applied on the fresh cut. Finally, the thickness of the undamaged layer was measured using a ruler. 12 measurement points were considered for each specimen.

A simple pattern matching technique is applied for 1D pulse-echo ultrasonic signals. The method uses the pattern matching technique to detect the optimum match between the measured and predicted ultrasonic signals of the reflected waves from the deteriorated concrete specimens, and thus determined the damage depth [25]. In this study the following objective function is maximized [38]:

$$\max\left(\frac{\sum_{k=0}^{N-1}\left[s(n+k)-\bar{s}(n)\right]\left[s_m(k)-\bar{s}_m\right]}{\left(\sum_{k=0}^{N-1}\left[s(n+k)-\bar{s}(n)\right]^2\right)\left(\sum_{k=0}^{N-1}\left[s_m(k)-\bar{s}_m\right]^2\right)}\right),\qquad(6)$$

where $\bar{s}(n)$ and $\bar{s}_m(n)$ are the sample means of the experimental and modeled signals in the time domain. The 1D multi-layer model is used for the signal modelling. The maximized term represents the centered correlation coefficient.

The phenolphthalein test results are presented with the ultrasonic thickness estimation data and data obtained by the pattern matching technique in Fig. 9 for the single-sided deteriorated specimens. The experimental results show very good correspondence of all three techniques used for the undamaged concrete thickness estimation: the pulse-echo ultrasonics, the phenolphthalein test and the pattern matching technique.

The pattern matching is performed for each ultrasonic signal from the corresponding B-scan data which also is used for estimation of the time of flight of ultrasonic signals employing Eq. (2). The estimated results show very good agreement between the pattern matching from both sides: undamaged and deteriorated. The difference between the corresponding averaged values is less than
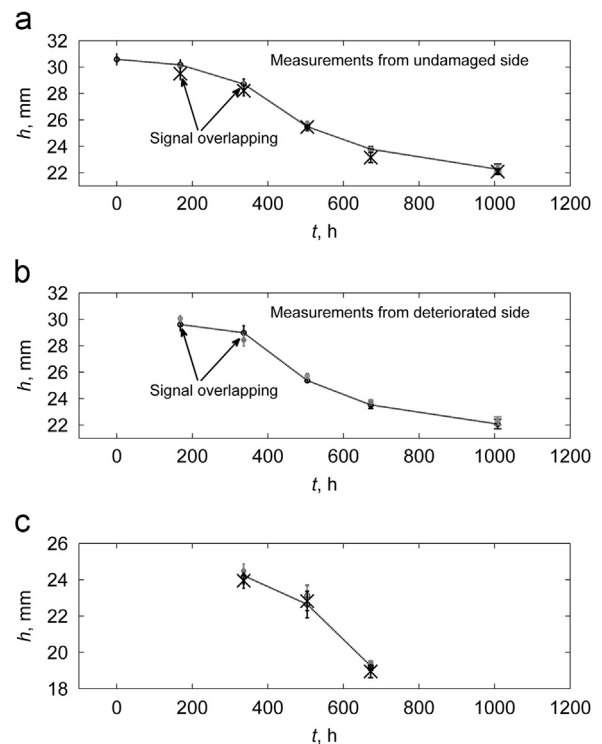

Fig. 9. Undamaged concrete layer thickness estimation by the three different techniques: the pulse-echo ultrasonics (black curve), the phenolphthalein test (black cross points) and the pattern matching technique (gray points). The results are presented for the measurement case from the undamaged (a) and deteriorated (b and c) sides of concrete.

0.05 mm. Also, the pattern matching technique demonstrates a low scattering. The scattering is less than ± 0.5 mm in the worst case. The direct thickness measurements by the pulse-echo technique using the time of flight of ultrasonic pulses provide a higher difference between the measurement results. For details, see Fig. 6(a).

The phenolphthalein test results and the pattern matching results for the double-sided deteriorated concrete specimens are depicted in Fig. 9(c). In this case the pattern matching is performed using the predicted signals for the double-sided symmetrically deteriorated concrete, i.e. the predictions are not performed separately for the double-sided deteriorated specimens with the anti-symmetric deterioration. Therefore, the objective function (Eq. 6) is calculated rejecting reflected ultrasonic pulsed from the top and bottom walls. The mismatch between the phenolphthalein test results and the ultrasonic results is larger than in the previous case (see Fig. 9(a)). Two dominant reasons for the mismatch are: (1) the local phenolphthalein test is performed on the edge of the specimens (20 mm width from edge was cut), therefore the deterioration depth is not verified along the length of the concrete specimens. The ultrasonic measurements are performed along the specimens. (2) The phenolphthalein tests are subjective, because the remaining thickness of the undamaged concrete is measured by a ruler and it is difficult to estimate true boundaries for the undamaged concrete. The estimation accuracy is ± 0.4 mm.

9. Conclusions

This study presents numerical and experimental investigations of ultrasonic measurements with applications to estimate the undamaged concrete layer thickness in a deteriorated concrete structure. The numerical studies show that a simple 1D plane wave propagation model, based on the stiffness matrix method [33], is a suitable method to model and predict ultrasonic wave propagation in deteriorated concrete structures. The ultrasonic predictions are verified by ultrasonic experiments and phenolphthalein tests.

Experimental pulse-echo ultrasonic measurements of the undamaged concrete layer thickness show that these measurements are reliable when the thickness of the deteriorated layer is large than the wavelength of acoustic wave. It is shown experimentally that the measurement results have low scattering: (a) ± 0.5 mm for the single-sided deteriorated specimens, and (b) ± 0.74 mm for the double-sided deteriorated specimens when the pulse-echo measurements are used. The use of shorter wavelengths is limited by the high acoustic losses which are present in the deteriorated concrete structures. Two different approaches are presented in this study to overcome this limitation: (1) a diffuse field technique, (2) a pattern matching approach. The first approach becomes attractive when it is not possible to predict a measurement situation or predictions are too complex. However, in this case it is necessary to find signal features which correlate well with the thickness of the undamaged or damaged concrete structure. In this study the diffuse field technique is presented as complementary/alternative to the pulse-echo measurements. The experimental results show that this technique works well when the deterioration depth of the concrete is smaller or/and comparable with the wavelength. By combining the pulse-echo and diffuse field measurement techniques, both minor and major deterioration levels can be detected and quantified. Furthermore, the location of the deterioration (inner shell, outer shell or both) can be determined. However, for the absolute thickness estimation from the diffuse field measurements, it is necessary to use calibration curves, which can be developed prior to the field measurements.

It is shown that the predicted signals can be used in the pattern matching approach. This technique is very useful when signal overlapping occurs in the pulse-eco measurements. It is experimentally shown that the pattern matching technique provides comparable results with the direct ultrasonic measurements. Alternatively to the pattern matching technique, it is possible to invert a full structure geometry (number and thickness of layers) with corresponding material properties using a global optimization technique [39]. However, this process is iterative, hence is computationally expensive.

Longitudinal wave phase velocity dispersion is measured in undamaged and deteriorated concrete specimens. The measurement results show that the phase velocity has very little dispersion in the deteriorated concrete and the velocity is 1625 m/s approximately in the measured frequency range 0.2–1 MHz.

References

[1] Slaats PG, Mesman GA, Rosenthal LP, Brink H. Tools to monitor corrosion of cement-containing water mains. Water Sci Technol 2004;49:33–9.
[2] Liu Z, Kleiner Y, Rajani B, Wang L, Condit W. Condition assessment technologies for water transmission and distribution systems. Technical report, EPA/600/R-12/017, USA; 2012.
[3] Gucunski N, Imani A, Romero F, Nazarian S, Yuan D, Wiggenhauser H, Shokouhi P, Taffe A, Kutrubes D. Nondestructive testing to identify concrete bridge deck deterioration. Technical report, SHRP 2 Report S2-R06A-RR-1, USA; 2013.
[4] Fan YF, Hu ZQ, Zhang YZ, Liu JL. Deterioration of compressive property of concrete under simulated acid rain environment. Constr Build Mater 2010;24:1975–83.
[5] Jones R. The ultrasonic testing of concrete. Ultrasonics 1963;1:78–82.
[6] Ould Naffa S, Goueygou M, Piwakowski B, Buyle-Bodin F. Detection of chemical damage in concrete using ultrasound. Ultrasonics 2002;40:247–51.
[7] Gudra T, Stawiski B. Non-destructive strength characterization of concrete using surface waves. NDT&E Int 2000;33:1–6.
[8] Cho YS. Non-destructive testing of high strength concrete using spectral analysis of surface waves. NDT&E Int 2003;36:229–35.
[9] Bracken M, Johnston D, Coleman M. Asset management of asbestos cement pipes using acoustic methods: Theory and case studies. In: Proceedings of the Pipelines Conference: A Sound Conduit for Sharing Solutions; 2011. pp. 225–235.
[10] Iyer S, Sinha SK, Pedrick MK, Tittmann BR. Evaluation of ultrasonic inspection and imaging systems for concrete pipes. Automat Constr 2012;22:149–64.
[11] Nayfeh AH. Wave propagation in layered anisotropic media. Amsterdam: Elsevier Publication; 1995.
[12] Antonaci P, Bruno CLE, Gliozzi AS, Scalerandi M. Monitoring evolution of compressive damage in concrete with linear and nonlinear ultrasonic methods. Cement Concrete Res 2010;40:1106–13.
[13] Liu M, Tang G, Jacobs LJ, Qu J. A nonlinear wave mixing method for detecting Alkali-Silica reactivity of aggregates. In: Proceedings of the AIP Conference; 2012. 1430. pp. 1524–31.
[14] Anugonda P, Wiehn JS, Turner JA. Diffusion of ultrasound in concrete. Ultrasonics 2001;39:429–35.
[15] Becker J, Jacobs LJ, Qu J. Characterization of cement-based materials using diffuse ultrasound. J Eng Mec-ASCE 2003;129:1478–84.
[16] Larose E, Planes T, Rossetto V, Margerin L. Locating a small change in a multiple scattering environment. Appl Phys Lett 2010;96:204101–1–204101-3.
[17] Quiviger A, Payan C, Chaix J-F, Garnier V, Salin J. Effect of the presence and size of a real macro-crack on diffuse ultrasound in concrete. NDT&E Int 2012;45:128–32.

[18] Ramamoorthy SK, Kane Y, Turner JA. Ultrasound diffusion for crack depth determination in concrete. J Acoust Soc Am 2004;115:523–9.

[19] Deroo F, Kim J-Y, Qu J, Sabra K, Jacobs LJ. Detection of damage in concrete using diffuse ultrasound. J Acoust Soc Am 2010;127:3315–8.

[20] Schurr DP, Kim J-Y, Sabra KG, Jacobs LJ. Damage detection in concrete using coda wave interferometry. NDT&E Int 2011;44:728–35.

[21] Payan C, Garnier V, Moysan J, Johnson PA. Determination of third order elastic constants in a complex solid applying coda wave interferometry. Appl Phys Lett 2009;94:011904–1–011904-3.

[22] Croxford AJ, Wilcox PD, Drinkwater BW, Nagy PB. The use of non-collinear mixing for nonlinear ultrasonic detection of plasticity and fatigue. J Acoust Soc Am 2009;126:EL117–22.

[23] Demčenko A, Koissin V, Korneev VA. Noncollinear wave mixing for measurement of dynamic processes in polymers: physical ageing in thermoplastics and epoxy cure. Ultrasonics 2014;54:684–93.

[24] Chang C-F, Chen J-W. The experimental investigation of concrete carbonation depth. Cement Concrete Res 2006;36:1760–7.

[25] Islam MM, Yamamoto H, Tanaka S. Non-destructive inspection of multiple concrete cracks using ultrasonic sensor. In: Proceedings of the SICE-ICASE International Joint Conference; 2006. pp. 5797–805.

[26] Mordak J, Wheeler J. Deterioration of asbestos cement water mains. Wiltshire: Water Research Center; 1988 Technical report.

[27] Zivica V, Bajza A. Acidic attack of cement based materials-A review. Part 1. Principle of acidic attack. Constr Build Mater 2001;15:331–40.

[28] Huang P, Bao Y, Yao Y. Influence of HCl corrosion on the mechanical properties of concrete. Cement Concrete Res 2005;35:584–9.

[29] Carde C, François R. Effect of the leaching of calcium hydroxide from cement paste on mechanical and physical properties. Cement Concrete Res 1997;27:539–50.

[30] Sachse W, Pao YH. On the determination of phase and group velocities of dispersive waves in solids. J App Phys 1978;49:4320–7.

[31] Lee KI, Humphrey VF, Kim B-N, Yoon SW. Frequency dependencies of phase velocity and attenuation coefficient in a water-saturated sandy sediment from 0.3 to 1.0 MHz. . J Acoust Soc Am 2007;121:2553–8.

[32] Zhang C, Le LH, Zheng R, Ta D, Lou E. Measurements of ultrasonic phase velocities and attenuation of slow waves in cellular aluminum foams as cancellous bone-mimicking phantoms. J Acoust Soc Am 2011;129:3317–26.

[33] Rokhlin SI, Wang L. Stable recursive algorithm for elastic wave propagation in layered anisotropic media: stiffness matrix method. J Acoust Soc Am 2002;112:822–34.

[34] Hosten B. Bulk heterogeneous plane waves propagation through viscoelastic plates and stratified media with large values of frequency domain. Ultrasonics 1991;29:445–50.

[35] Ingle VK, Proakis JG. Digital Signal Processing Using MATLAB. 3rd edCengage Learning; 2012.

[36] Demčenko A. Non-collinear wave mixing for a bulk wave phase velocity measurement in an isotropic solid. In: Proceedings of the IEEE International Ultrasonics Symposium; 2012. pp. 1437–40.

[37] Michaels JE, Michaels TE. Detection of structural damage from the local temporal coherence of diffuse ultrasonic signals. IEEE Trans Ultrason Ferroelectr Freq Control 2005;52:1769–82.

[38] McNames J. Fast algorithms for computing similarity measures in signals. In: Lyons RG, editor. Streamlining digital signal processing: A tricks of the trade guidebook. Hoboken: John Wiley & Sons Inc;; 2007. p. 117–26.

[39] Castaings M, Hosten B, Kundu T. Inversion of ultrasonic, plane-wave transmission data in composite plates to infer viscoelastic material properties. NDT&E Int 2000;33:377–92.